Vol. 203, No. 1, 1994 BIOCHEMICAL AND BIOPHYSICAL RESEARCH COMMUNICATIONS
August 30, 1994 Pages 331-337

CYTOCHROME *c* OXIDASE IN PROTEOLIPOSOMES VISUALISED BY PLATINUM-CARBON AND BY TUNGSTEN-TANTALUM SHADOWING: IMAGE ANALYSIS

Mariana Tihova#, Brenda Tattrie and Peter Nicholls*

Dept. Biological Sciences, Brock University, St. Catharines, ON L2S 3A1, Canada

Received June 28, 1994

Summary: Beef heart cytochrome *c* oxidase complexes incorporated into phospholipid liposomes were examined by freeze-fracture electron microscopy. Enzyme molecules are inserted into the membrane asymmetrically, with larger projections on the 'C' side, where cytochrome *c* binding occurs, than on the 'M' (matrix-facing) side. Visualisation of the complexes was improved by: (i) image analysis, to determine details of size and shape, and (ii) tungsten-tantalum (W/Ta) rather than platinum-carbon (Pt/C) shadowing, which permits examination of smaller entities. Enzyme molecules are incorporated as dimers in the proteoliposomes. Some surface structural details of the embedded molecules can be discerned. Around each complex is seen a small area of modified lipid, the frozen annulus whose existence has been predicted with other methods.

Eukaryotic cytochrome *c* oxidase, the terminal respiratory enzyme, is a protein with up to 13 peptides (1), which transfers electrons from the respiratory chain to molecular oxygen and at the same time pumps protons across the inner mitochondrial membrane in which it is embedded. Reconstituted cytochrome *c* oxidase has been the subject of several structural investigations (2-7). Sometimes (5), but not always (6), the embedded complexes are dimers.

We have previously studied monomer-dimer interconversion using conventional Pt/C replicas and image analysis (9). This paper reports the

#Present address: Dept. Psychology, Dalhousie University, Halifax, NS B3H 4J1, Canada.

*To whom correspondence should be addressed.

0006-291X/94 $5.00

results of tungsten-tantalum (W/Ta) shadowing, which in principle permits examination of much smaller entities (10). Use of this technique throws further light upon the arrangement of the enzyme across the membrane and on the relationship between the enzyme molecule and the sea of surrounding phospholipid (11,12).

Materials and Methods

Cytochrome *c* oxidase-containing vesicles (COV) were prepared by cholate dialysis using bovine heart enzyme with 1:1 (w:w) mixtures of egg phosphatidylcholine (EPC) / phosphatidylethanolamine (EPE) or dioleoyl-L-phosphatidylcholine (DOPC) dioleoyl-L-phospatidyl-ethanolamine (DOPE) at phospholipid to protein ratios (L:P) of 25 mg/mg and 10 mg/mg. The COV were fractionated on DEAE-Sephacel, as described in (9). Samples (0.1-0.2 mL) of the third, most tightly bound fraction (FIII) were rapidly spray frozen from 0°C on a Balzers Spray Freezing Unit and freeze-fractured using a Balzers 400T device with quartz crystal monitored shadowing, forming replicas at -150°C and $5x10^{-6}$ Pa. W/Ta shadowing was performed in four to six steps, each lasting 3 seconds, separated by 10 second periods during which the partly shadowed surfaces were allowed to cool. To avoid contamination of fractured surfaces, samples were protected between each shadowing step by the liquid nitrogen cooled knife (9). Photomicrographs were prepared with a Philips 300 electron microscope. Video images (negatives) were digitized using the BRS or M1 software packages in the MCID system of Imaging Research Inc., Brock University. Images were photographed from the screen image or stored as TIF files and printed with a Hewlett-Packard Laserwriter from a suitable graphics package.

Results

Figure 1 shows a digital screen image of a Pt/C COV replica. The projecting particles indicate locations and shapes of the original oxidase molecules. The particle areas and the size distribution profiles were calculated, correcting the data for each projection for the contribution of the Pt grains involved (as described in ref. 9). The size distribution profiles are summarised in Table 1, which lists the results of measurements on convex surfaces of EPC/EPE and DOPC/DOPE COV at the two L:P ratios. The populations showed certain discrete values. Particles with average areas of 70 nm^2 on the C-side and 40 nm^2 on the M-side represent oxidase dimers (9). The 70 nm^2 particles are outward-facing dimers, and the 40 nm^2 particles mainly inward-facing dimers (9).

Fig. 2A shows the digitized screen image produced for a similar cytochrome *c* oxidase-containing proteoliposome by W/Ta shadowing. Its

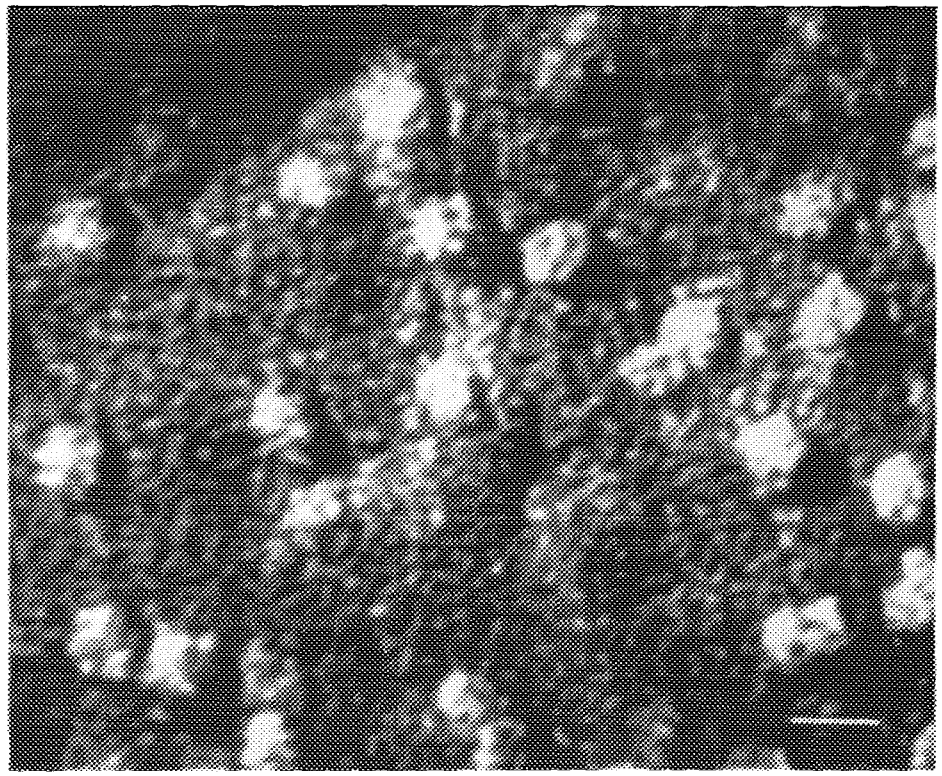

Figure 1. Digitized image of a Pt/C replica of eggPC/eggPE proteoliposomes. The projecting particles are oxidase complexes. Particle areas were determined with the image analysis system. Size bar = 10 nm.

TABLE 1. POPULATION PERCENTAGES FOR CYTOCHROME *c* OXIDASE OLIGOMERS IN FOUR COV TYPES : IMAGE ANALYSIS OF Pt/C REPLICAS

Average area of particle population*	DOPC/DOPE COV		EggPC/PE	
	L:P=10**	L:P = 25**	L:P=10**	L:P=25**
40 $nm^{2\#}$	38%	41%	13%	22%
70 $nm^{2\#\#}$	33%	36%	25%	34%
100 $nm^{2\#\#\#}$	14%	10%	31%	23%
140 $nm^{2\#\#\#}$	2%	11%	20%	13%

* convex faces (presumed exterior faces), obtained by image analysis from figures such as Fig. 1. The areas of the covering Pt particles were deducted from the totals in order to arrive at the final calculated values (9).

** Phospholipid:protein ratios (weight/weight).

\# Smaller areas = M (matrix) faces of dimers or C faces of monomers.

\#\# Larger areas = C (external or cyt. *c*-binding) faces of dimers.

\#\#\# Tetramers and larger aggregates (M and C faces).

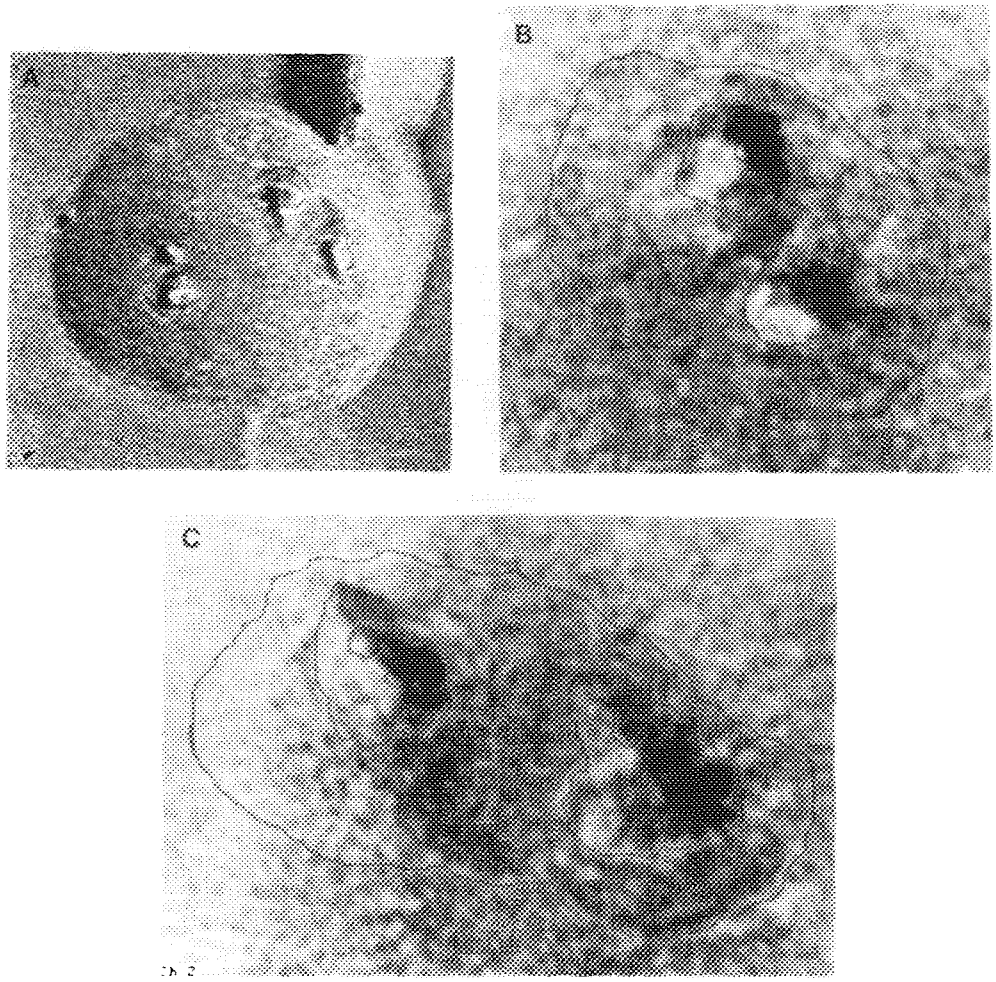

Figure 2. Protein projections in W/Ta shadowed replicas of cytochrome *c* oxidase-loaded proteoliposomes.

A. A digitized image of the convex surface of the whole proteoliposome (eggPC/eggPE plus cytochrome oxidase). The four components organized as two doublets were chosen for presentation in **B** & **C**. Size bar = 10nm.

B. A digitized image of the two quasisymmetrical components of the first of the two doublets from Fig. 2A. The projecting areas are between 45 & 65 nm^2, and the areas of the smaller projections in the centers of the structures are 2.5 and 3.5nm^2. The outlined area of phospholipid membrane showing a different texture from the rest of the liposome surface, and with a distinct boundary, occupies 400nm^2 in addition to the area of the two projections.

C. A digitized image of the two elongated components of the second doublet shown in Fig. 2A. The large projecting areas have areas of 75-110 nm^2 and 100-150 nm^2, respectively. The areas of the four smaller projections lie between 3.2 nm^2 and 5.4 nm^2. The 'internal' distances between the members of these small pairs are 5.3 nm and 4.1 nm. The surrounding modified lipid area, common to both components, occupies nearly 600 nm^2 in addition to the area of the projections.

convex surface contains four projecting components, organized as two doublets. Fig. 2B shows the details of one of the pairs. The two enzyme projections cover areas of about 45nm^2 (minimum) and 60nm^2 (maximum). These values are greater than the areas of the smaller projections in Pt/C replicas (9). The two components of the doublet are separated by 16 nm. Each is rather symmetrical, and each component contains a small projecting region with an area of 2.5 - 3.5 nm^2. This region may indicate one subdomain in the oxidase molecule (5). The whole complex is embedded in 400 nm^2 of phospholipid which has a modified surface texture. If each phospholipid molecule occupies an area of 0.6 nm^2, the 400 nm^2 area of modified lipid structure contains 700 lipid molecules. If the outlined structures are C-faces of oxidase monomers, about 350 modified phospholipid molecules are thus associated with each monomer.

Fig. 2C shows a digitized image of the second doublet. The area of each of its two components is approximately 100 nm^2. This is greater than the corrected C-face areas of the dimers (9), and these components may thus represent dimers with assymmetrical elongated shapes. The component monomers may be represented by the two smaller projecting round subregions separated within the complexes. The surrounding phospholipid area with modified texture common to the whole complex is 600 nm^2. This special area thus contains 1000 phospholipid molecules, 250 molecules/monomer. Each component is crowned with a pair of smaller projections with areas of 3.2 to 5.4 nm^2. The centre to centre distances of these sub-projections are between 4.0 and 5.5 nm.

Discussion

Falk and Karlson (11) reported that immobilised phospholipid occurs in oxidase vesicles prepared with egg PC. Each incorporated cytochrome *c* oxidase monomer prevents 100 lipid molecules from participating in the main gel-liquid-crystalline transition (12). The 'annulus' phospholipid may remain in the same physical state below and above the main transition temperature, providing a nearly constant microenvironment for the protein. Phospholipid hydrocarbon chain mobility is substantially reduced as protein concentration increases (13). Exchange of lipid between the restricted and the more mobile phases occurs on a millisecond or longer time scale. Estimates of 90 to 100 bound molecules of phospholipid per protein complex were also obtained from the dependence of protein mobility on the lipid:protein ratio (14). To describe the relationship between protein and membrane lipid, Bloom and coworkers (15) developed

a 'mattress' model, in which the lengths of the phospholipid hydrocarbon chains adapt to the transmembrane length of the hydrophobic portions of the protein.

In these measurements and theoretical models the quantity of closely associated lipid is much less than in the perturbed area of bilayer in our W/Ta shadowed preparations. The freeze-fracture W/Ta method may exaggerate the size of the "immobilised" region of phospholipid on both sides of the membrane surrounding the cytochrome oxidase complexes. W/Ta shadowing gives larger areas for the enzyme particles, consistent with the expected values (3, 5, 12) for oxidase dimers seen from the two sides (C and M), and greater than those obtained by Valpuesta *et al.*(7) using cryoelectron microscopy and Ruben *et al.*(8).

The difference in size distributions for egg phospholipid compared with the dioleoyl phospholipid (9) indicates that phospholipid composition has a significant effect upon enzyme incorporation, conformation, and aggregation state. DOPC/DOPE bilayers are more fluid than those of eggPC/PE, which favours more disorder during enzyme incorporation but also less particle aggregation.

Some substructures (3 to 5 nm subdomains), whose existence was predicted by previous methods, can now be seen directly. Unfortunately the resolution of the improved method still does not extend below the 1 to 2 nm range. For an 'in depth' structural determination we must still await preparation of genuine three-dimensional crystals of this important macromolecule (16,17).

Acknowledgments. This work was supported by Canadian NSERC operating grant A-0412 and equipment grants to P.N. We thank Drs. John Wrigglesworth of King's College, London, and Peter Rand, of Brock University, for discussions of freeze-fracture electron microscopy and Ms. Nola Fuller of this university for assistance with replica preparation and analysis.

References

1. Wrigglesworth, J. M., Wooster, M. S., Elsden, J., & Danneel, H.-J. (1987) Biochem. J. **246**, 737-744.

2. Hinkle, P. C., Kim, J. J., & Racker, E. (1972) J. Biol. Chem. **247**, 1338-1339.

3. Costello, M., & Frey, T. (1982) J. Mol. Biol. **162**, 131-156.

4. Cooper, C., & Nicholls, P. (1990) Biochemistry **29**, 3865-387.

5. Frey, T., Costello, M., Karlsson, B., Haselgrove, J., & Leigh J. (1982) J. Mol. Biol. **162**, 113-130.

6. Nalecz, K., Bolli, R., Ludwig, B., & Azzi, A. (1985) Biochim. Biophys. Acta **808,** 259-272.

7. Valpuesta, J., Henderson, R., & Frey, T. (1990) J. Mol. Biol. **214**, 237-251.

8. Ruben, G. and Teiford, J. (1980) J.Microsc. **118**, 1191-216.

9. Tihova, M., Tattrie, B. & Nicholls, P. (1993) Biochem. J., **292**, 933-946.

10. Rigaud, J., Gulik-Krzywicki, T. & Seigneuret, M. (1988) *in* The Ion Pumps: Structure, Function, and Regulation (ed. W.D.Stein), pp.99-104., Alan R. Liss.

11. Falk, K. & Karlsson, B. (1979) FEBS Letters **98**, 25-27.

12. Rigell, C., de Saussure, C. & Freire, E. (1985) Biochemistry, **24**, 5638-5646.

13. Longmuir, K., Capaldi, R. & Dahlquist, F. (1977) Biochemistry, **16**, 5746-5755.

14. Fajer, P., Knowles, P. & Marsh, D. (1989) Biochemistry, **28**, 5634-5643.

15. Bloom, M., Evans, E., & Mouritsen, O. (1991)Quart. Rev. Biophys., **24**, 293-397.

16. Zamudio, I., Kornblatt, J., Nicholls, P. Li, Y. & Cygler, M. (1990) Biochem. Biophys. Res. Comm. **169**, 1105-1110.

17. Kühlbrandt, W. (1992) Quart. Revs. Biophys. **25**, 1-49.